Submitted in the ApJ on April 15, 2003
Preprint typeset using LaTeX style emulateapj v. 11/12/01

COMPARING CHANDRA AND SIRTF OBSERVATIONS FOR OBSCURED STARBURSTS AND AGN AT HIGH REDSHIFT

D. Weedman, V. Charmandaris[1]
Astronomy Department, Cornell University, Ithaca, NY 14853
dweedman@isc.astro.cornell.edu,vassilis@astro.cornell.edu

A. Zezas
Harvard-Smithsonian Center for Astrophysics, 60 Garden Street, Cambridge, MA 02138
azezas@head-cfa.harvard.edu
Submitted in the ApJ on April 15, 2003

ABSTRACT

Tracking the star formation rate to high redshifts requires knowledge of the contribution from both optically visible and obscured sources. The dusty, optically-obscured galaxies can be located by X-ray and infrared surveys. To establish criteria for selecting such sources based only on X-ray and infrared surveys, we determine the ratio of infrared to X-ray brightness that would be observed by SIRTF and Chandra for objects with the same spectral shapes as nearby starbursts if seen at high redshift. The parameter IR/X is defined as IR/X = (flux density observed in SIRTF MIPS 24 μm filter in mJy)/(total flux observed within 0.5–2.0 keV in units of 10^{-16} ergs s^{-1} cm^{-2}). Based on observations of NGC 4038/39 ("The Antennae"), NGC 3690+IC 694 (Arp 299 or Mkn 171), M 82, and Arp 220, nine starburst regions are compared using mid-infrared spectra taken by the Infrared Space Observatory (ISO) and X-ray spectra obtained with Chandra . The IR/X are determined as they would appear for $1 < z < 3$. The mean IR/X over this redshift range is 1.3 and is not a significant function of redshift or luminosity, indicating that SIRTF surveys reaching 0.4 mJy at 24 μm should detect the same starbursts as deep CXO surveys detect at a flux of 0.3×10^{-16} ergs s^{-1} cm^{-2}. The lower bound of IR/X for starbursts is about 0.2, suggesting that objects with IR/X smaller than this have an AGN X-ray component in addition to the starburst. Values of IR/X for the obscured AGN within NGC 1068, the Circinus galaxy, and NGC 6240 are also determined for comparison although interpretation is complicated by the circumnuclear starbursts in these galaxies. Any sources found in surveys having IR/X>4 would not match any of the objects considered.

Subject headings: dust, extinction — galaxies: high-redshift – infrared: galaxies — X-rays: galaxies — galaxies: AGN — galaxies: starburst

1. INTRODUCTION

Understanding the formation and evolution of galaxies requires measuring the star formation rate as a function of redshift in the universe. Currently available data indicate that the star formation rate was much greater at z∼1 than at the present, but whether this rate continues to increase or stabilizes for z>1 is essentially unknown (Chary & Elbaz 2001). An equally crucial issue is understanding the development and evolution of active galactic nuclei (AGN) and how this relates to star and galaxy formation. An important challenge for these questions is to determine the fraction of sources that are so obscured by dust that they have not been accounted for in optical surveys. Such objects are probably the dominant source of observed background emission at infrared and submillimeter wavelengths and seemingly comprise the majority of the luminosity density in the universe (e.g. Hauser et al. 1998; Barger, Cowie, & Richards 2000). Even when optically obscured, dusty sources can be selectively located by X-ray surveys and by infrared surveys. In X-rays, radiation from the primary source can be seen directly as long as the HI column density of the obscured region is less than $\sim10^{24}$ cm^{-2} or can be seen in X-rays scattered outside the obscuring region. In the infrared, dust is seen via direct emission of infrared luminosity; this luminosity arises from reradiation by the dust of energy initially emitted as X-ray, ultraviolet and visible photons.

It is established already from deep surveys with the Chandra X-ray Observatory (CXO) that a substantial population of objects exist which are too faint for optical spectroscopic redshift determination. For example, about 10% of the sources in the Chandra Deep Field-North survey (CDF-N) are optically blank, with R>26.5 mag (Hornschemeier et al. 2001). These may be optically faint because of obscuration by dust, which becomes even more significant at high redshift when the observed optical wavelength corresponds to ultraviolet wavelengths in the source rest frame. The CDF-N has also shown that CXO sources are often the same as infrared sources found in deep surveys with the Infrared Space Observatory (ISO) (Alexander et al. 2002). In the overlapping survey area (about 22 arcmin^2, or 5% of the CDF-N area), there are 41 ISO sources and 49 CXO sources, and about one-third of these are seen by both. This is an important indication that both X-ray and infrared surveys are crucial in identifying dust enshrouded distant galaxies.

The next opportunity for major progress in infrared surveys will be with the Space Infrared Telescope Facility (SIRTF)[2]. It is the intention with SIRTF to undertake sur-

[1] Chercheur Associé, Observatoire de Paris, LERMA, 61 Av. de l'Observatoire, F-75014 Paris, France
[2] Information on SIRTF is at http://sirtf.caltech.edu/SSC/

veys that can detect infrared sources over areas of many square degrees, and all of the CXO deep fields are planned to be covered by SIRTF. Because CXO and SIRTF will continue simultaneous operation for many years, it is probable that numerous regions of the extragalactic sky will be imaged both in X-rays and infrared. SIRTF will readily extend to higher redshifts the infrared census previously determined by ISO. SIRTF surveys will be especially sensitive to dusty starbursts because of the strong suite of spectral features between 6 and 13 μm rest wavelength arising from molecular emission by polycyclic aromatic hydrocarbons (PAH), features which are very strong in starbursts (e.g. Figure 2). These emission features are so strong that an object can appear many times brighter in images at wavelengths centered on this emission than in images at continuum wavelengths. For example, the strong 7.7 μm feature made the extensive surveys by ISOCAM at 15 μm particularly sensitive to starburst galaxies at z$\sim$1 (Elbaz et al. 2002). The analogous SIRTF surveys will be at 24 μm, using the Multiband Imaging Photometer (MIPS), and will readily reach survey limits of 0.4 mJy in large area, shallow surveys (Dole, Lagache, & Puget 2003). This will allow the extension to z$\sim$3 of the luminosity function for dusty starbursts tracked to z$\sim$1.2 by ISO. For obscured starbursts too faint for optical redshift determination, the Infrared Spectrograph on SIRTF will be able to determine redshifts to z$\sim$4 based on the strong PAH features.

Both AGN and starbursts produce copious X-ray and infrared emission, but for dramatically different reasons. Hard X-rays arise from hot accretion disks near massive black holes in AGN, but in starburst galaxies they originate from accretion disks near compact stellar remnants; the summed contribution of these individual sources makes starbursts a significant source of hard X-rays. Soft X-rays arise from hot winds flowing from accretion disks in AGN but also arise from young stars, stellar winds, and supernova remnants in starbursts. Dust reradiation comes from dust grains and molecules which are either heated or photoexcited by the radiation from accretion disks in AGN, or from hot stars in starbursts. While it is often assumed that most extragalactic X-ray sources are AGN, it is known that ultraluminous starburst galaxies can be significant X-ray sources even at high redshift (e.g. Moran, Lehnert, & Helfand 1999; Zezas et al. 1998; Hornschemeier et al. 2002), and the majority of faint sources with both CXO and ISO detections have been interpreted as starburst galaxies rather than AGN (Alexander et al. 2002). It is important to determine how the comparison of SIRTF and CXO surveys can locate those luminous, dusty sources powered primarily by starbursts and distinguish them from sources powered by AGN.

The redshift interval 1<z<3 is particularly crucial to explore for several reasons. It is known from optical surveys that this is the interval in which the optically discoverable quasar luminosity function peaks (Fan et al. 2001). It might be expected, therefore, that significant numbers of X-ray selected AGN would also be found at these redshifts, and the X-ray surveys should detect any significant population of obscured sources. This is also the interval in which modeling of infrared source counts implies that ultraluminous infrared galaxies powered by starbursts reach their peak (Xu et al. 2003). Determining luminosity functions out to z$\sim$3 that include obscured sources is the only way to determine when both star formation and AGN activity peaked in the universe. There are adequate reasons to expect that SIRTF will detect many sources at z>1. Various infrared and submillimeter observations demonstrate that ultraluminous infrared galaxies (ULIRGs) exist with bolometric luminosities about $10^{13}\,L_\odot$. Source counts and evolution deduced from background constraints require that such sources are hundreds of times more common per unit volume at z>2 than in the local universe (e.g. Lagache, Dole, & Puget 2003). Taking the spectral energy distribution of a $10^{13}\,L_\odot$ galaxy from Chary & Elbaz (2001) along with their cosmological assumptions, the observed flux density at 24 μm for z=2 would be 2.7 mJy (enhanced by a strong PAH feature); at z=3, this flux density would be 0.4 mJy. Because SIRTF surveys will readily detect sources to these flux limits, SIRTF will have the potential to produce a luminosity function for obscured sources within a redshift range that is crucial for tracing ULIRGs at redshifts around the star-formation peak. It is important to determine how these ULIRGs might relate to faint, high redshift sources revealed in X-ray surveys and to learn if there is a selection criterion to distinguish between starburst and AGN as the dominant power source. Using comparisons of infrared and X-ray observations to consider this question is the objective of the current paper.

A necessary step toward using comparisons of infrared and X-ray measurements for studying the high redshift universe is to determine the relative "K-corrections" in the different wavelength regimes, because rest-frame emissions are found at significantly different observed wavelengths at high redshift. For example, by z=2, the CXO "soft band" (0.5–2.0 keV) actually samples the rest-frame energies of 1.5–6 keV. The deepest dust-sensitive surveys by SIRTF will be at an observing wavelength of 24 μm, corresponding to rest frame of 8 μm for z=2. To determine criteria for comparing CXO and SIRTF sources for the purpose of identifying candidate high redshift starburst galaxies, and for comparing starbursts with AGN, we need to know the characteristics of pure starbursts in the X-ray and infrared spectral regimes over broad enough wavelength ranges to determine relative K-corrections. To accomplish this, we consider in this paper a detailed comparison of the X-ray (from CXO) and infrared properties (from ISO) in the best examples of nearby, pure starbursts which have observations extending to the higher X-ray energies and shorter infrared wavelengths where such objects would be seen in the observer's frame at high redshifts. Our specific objective is to determine the range of infrared/X-ray ratios which should be observed for pure starbursts at various redshifts up to z=3, when observed in the CXO soft band, the most sensitive CXO band, and the SIRTF 24 μm MIPS band. By using known examples of local starbursts, these ratios can be determined empirically. We also use a more limited sample of obscured AGN as an initial step toward comparing them with starbursts.

2. CHOICE OF OBJECTS FOR STUDY

The "pure starburst" objects used for these infrared to X-ray comparisons are luminous galaxies in both X-ray and infrared for which careful multiwavelength studies have shown that they only harbor luminous starbursts

with no evidence for AGN activity. For our comparisons, we also require that adequate archival ISO and CXO data exist in order to determine what the infrared/X-ray ratio would be if observed at various redshifts. Our approach is strictly empirical, so we desire to include objects with a variety of morphologies and luminosities, including nuclear starbursts, entire interacting systems, and individual starbursts within galaxies. For the distant objects to be sought with SIRTF surveys, the spatial resolution will not be adequate to distinguish among these different types of starbursts based on morphology.

Archival data are now available from CXO and ISO for a number of local starburst galaxies for which spectral data can be extracted from spatial areas identical in both X-ray and infrared. The objects used in the present paper are the interacting system NGC 3690+IC 694 (also Markarian 171 or Arp 299), the interacting system NGC 4038+NGC 4039 (also the "Antennae"), the prototypical starburst galaxy M 82, and Arp 220, the prototypical ULIRG. Taking this collection of objects, we will be able to describe the infrared/X-ray ratios of 9 different starburst regions with sufficient spectral coverage to describe how they would appear if they were located at 1<z<3. The regions used cover a luminosity range approaching 100 and thus will allow investigation of whether the ratio depends on luminosity. ISOCAM 15 μm images of the sources showing the spatial regions compared in infrared and X-ray are shown in Figure 1. The appearance of these regions in X-rays depends on the energy, and representative images illustrating this are cited below in discussions of individual objects.

1. NGC 3690 + IC 694: These combined objects comprise the system Arp 299 or Markarian 171 which has long been interpreted as a luminous starburst galaxy (Gehrz, Sramek & Weedman 1983). Careful studies utilizing multiwavelength capabilities including HST have verified that virtually all of the luminosity at all wavelengths arises from multiple starbursts and their consequences (Zezas et al. 1998; Alonso-Herrero et al. 2000; Charmandaris, Stacey, & Gull 2002). ISO observations of this system have sufficient spatial resolution to isolate numerous starbursts for potential comparison with CXO observations (Gallais et al. 1998). An X-ray image showing the dramatic difference in appearance between soft band and hard band X-rays is in Zezas, Ward, & Murray (2003). We analyze three separate regions for this system: the components NGC 3690 and IC 694, and the total system. Even though the total system includes the other two regions, the system luminosity also includes extended emission which is outside of the smaller regions, so the extended total system is considered as a separate starburst region. Although recent observations with Beppo Sax at very high energy X-rays (>10 keV) reveal evidence for an AGN that may account for a few percent of the bolometric luminosity (Della Ceca et al. 2002), this AGN is very weak in the CXO band and does not affect the measured spectrum and flux of NGC 3690, where it is located (Zezas et al. 2003). The regions defined for our infrared and X-ray measures are illustrated in Figure 1a. The distance adopted is 42 Mpc.

2. NGC 4038 + 4039: These objects comprise the "Antennae" system of interacting galaxies, which provides another dramatic illustration of how the X-ray morphology of a starburst system changes with energy (Fabbiano, Zezas, & Murray 2001; Fabbiano et al. 2003). The soft band (in the rest frame) reveals extended, diffuse emission, whereas hard bands show individual sources with little diffuse emission. Optical, infrared, and millimeter observations thoroughly demonstrate the starburst nature of all components of the system (Vigroux et al. 1996; Mirabel et al. 1998; Wilson et al. 2000), and there is no evidence for AGN activity anywhere within the system. To accommodate empirically the variety of morphologies, we examine 4 regions: the localized "Knot A", the nuclei of NGC 4038 and 4039, and the entire system. As in Arp 299, the additional extended emission outside of the localized regions makes it appropriate to consider the entire system as a separate starburst region. The regions defined for our infrared and X-ray measures are illustrated in Figure 1b. The distance adopted is 20 Mpc.

3. Arp 220: This luminous infrared source is often described as the nearest ULIRG, but detailed multiwavelength studies have found no evidence for an AGN (see Smith et al. 1998; Iwasawa et al. 2001), so it is considered as the most luminous local starburst (e.g. Sturm et al. 1996; Charmandaris et al. 1999; Clements et al. 2002). The luminosity is concentrated in the nucleus, so we compare X-ray and infrared results only for the nuclear region, illustrated in Figure 1c. The distance adopted is 76 Mpc.

4. M 82: This nearby galaxy has long been considered the prototype for an extended starburst (Rieke et al. 1980). The interpretation of the ISO mid-IR data used is presented by Förster Schreiber et al. (2003). CXO results are intriguing but problematical for our current analysis, because of the presence of a luminous, highly variable, hard source (Kaaret et al. 2001; Matsumoto et al. 2001). When in a high state, this dominates the X-ray luminosity of the galaxy. For our present analysis, we did not include this source. As a result, the X-ray fluxes which enter our calculations for M 82 in Table 1 could sometimes be a factor of two higher than listed. As discussed further in section 4, below, M82 would be more similar to other starbursts in IR/X if the high-state flux were included. Except for this single source, we compare X-ray and infrared results for the entire galaxy illustrated in Figure 1b. Although this region does not include the galactic superwind seen in soft X-rays (e.g. Watson et al. 1984; Strickland et al. 1997), our redshifted bands correspond to X-ray emission above 1 keV so the X-ray component seen in these bands is associated with the optical body of the galaxy covered by our aperture. The distance adopted is 3.3 Mpc.

3. ANALYSIS OF INFRARED AND X-RAY DATA

Because our approach is empirical, we undertake an analysis to produce results directly applicable to observed measurements from CXO or SIRTF, as would be derived from wide field imaging surveys. For CXO, results for the most sensitive observations are usually given as total flux in the soft band from 0.5 keV to 2 keV. For SIRTF, the most sensitive results for dust reemission from obscured regions will be flux densities in the 24 μm MIPS band. The ratio of infrared to X-ray brightness which we define in this paper to compare SIRTF and Chandra measurements is the parameter IR/X, defined as IR/X = (infrared flux density measured with MIPS 24 μm in mJy)/(total X-ray flux observed between 0.5 and 2.0 keV in units of 10^{-16}

ergs s^{-1} cm^{-2}). In order to determine IR/X as would be observed at different redshifts, the relevant bandpasses have to be transformed to the rest frame spectra of the sources used. The objects which we evaluate have X-ray and infrared spectra extending over sufficient wavelengths in the rest frame that IR/X can be determined for redshifts 1<z<3.

The infrared spectra have various strong features which are comparable in spectral width to the MIPS 24 μm filter bandpass. Because observed results are given as a flux density at a single wavelength, it is necessary to determine the flux density at the corresponding rest-frame effective wavelength of the filter. Spectra which make this possible are readily available from the ISO archive. The infrared observations used in this paper were obtained with ISOCAM (Cesarsky et al. 1996), a 32×32 pixel array on board the ISO satellite, as part of the CAMACTIV GTO Program (principal investigator, F. Mirabel). Spectral maps of a region around each target were created using the Continuously Variable Filter (CVF) covering the full wavelength range 5.1–16.3 μm with a spectral resolution of ∼40. For NGC 4038/39, Arp 220, and NGC 3690/IC 694, the total field was $48'' \times 48''$ with $1.5''$ pixels. For M 82, field size and pixel size were $92''$ and $3''$, respectively. The spatial regions measured are shown in Figure 1. In all cases, the FWHM of the PSF varied between $4''$ and $5''$. Data were analyzed with the CAM Interactive Analysis software (CIA[3]). Since one of us (VC) was involved in the analysis and publication of the ISO results of all galaxies included in our sample, the reduced ISO data and analysis techniques we used were the same as those of Vigroux et al. (1996) and Mirabel et al. (1998) for NGC 4038/39, Charmandaris et al. (1999) for Arp 220, Gallais et al. (1998) for NGC 3690/IC 694, and Förster Schreiber et al. (2003) for M 82. Spectra of all the sources are shown in Figure 2.

The parameter IR/X is measured in the observer's frame so is given by IR/X = $f_\nu(1+z)/f_x$. Here, f_ν is the flux density in the rest frame at the effective wavelength, λ_{eff}, observed with the SIRTF MIPS 24 μm filter for the z of interest. The f_x is the total X-ray flux within the rest-frame energy range of 0.5(1+z) keV to 2.0(1+z) keV. Using the ISOCAM CVF spectra, the 24 μm filter response[4] with all wavelengths divided by (1+z) is folded into the spectrum to determine λ_{eff} for various redshifts. The source f_ν is then measured as the flux density at this λ_{eff} in the ISOCAM spectra.

To determine f_x, each evaluation requires a different energy cut for the CXO data, defining bands in the galaxy rest frames which would correspond to 0.5–2.0 keV in the observer's frame for the different redshifts. For example, at z=2, the observed 0.5–2.0 keV soft band corresponds to an energy range of 1.5–6.0 keV in the rest frame. The f_x were measured by fitting spectra extracted from the CXO Advanced CCD Imaging Spectrometer (ACIS) observations of the sources, obtained from the CXO archive, and then calculating the total fluxes in the necessary bands from these spectra. The CXO data were analyzed following standard procedures (e.g. Zezas et al. 2002; Zezas, Ward, & Murray 2003) using the CIAO v2.3 data analysis tool suite. After screening for time intervals of high background, X-ray spectra were extracted within the same spatial regions as for the ISO spectra. Because these regions are large compared to the scale over which ACIS response varies, we created response files for smaller segments where the response is constant and subsequently combined these to create the final response matrix and ancillary response files for a given region. Spectral fitting was performed with the XSPEC v11.1 package. It is desired to have only observed fluxes as they emerge from the sources, so no corrections were applied for internal absorption within the sources, although we did correct for the Galactic HI column density along the line of sight to each galaxy (Stark et al. 1992). These Galactic corrections are negligible within the energy bands used.

Table 1 summarizes the infrared and X-ray observational results for λ_{eff}, f_ν, and f_x. The resulting IR/X are those which would be observed at the different redshifts listed for spectra having shapes in the infrared and X-ray like those of the various starburst sources utilized. These results are also displayed in Figure 3.

4. COMPARISON OF SIRTF AND CXO SURVEYS

The results in Table 1 and Figure 3 show the range of IR/X values as a function of redshift for the different starbursts which are analyzed. Table 2 summarizes the mean IR/X over all redshifts for the different sources along with the source luminosities in the 2–8 keV band (arbitrarily chosen for luminosity comparison since it represents the broadest bandpass utilized). Many different physical effects can influence IR/X in different starbursts. These effects include what fraction of total radiated luminosity is absorbed by dust, what fraction of bolometric luminosity emerges at the rest wavelength observed in the infrared, the nature of the X-ray sources compared to the sources powering the infrared, the shape of the intrinsic X-ray spectrum, and how much the X-rays are absorbed. We do not attempt to pursue the implications of any of these results as might regard the physical nature of starbursts. Our objective is strictly to present empirical criteria as a baseline for future analysis of other sources.

The most important empirical results are: (a) The IR/X is not a significant function of redshift, except for redshift of z=2, where the strong 7.7 μm PAH feature produces significant additional flux density within the 24 μm filter band. (b) The IR/X is also not a function of luminosity; for example, NGC 4039 and Arp 299 starbursts have very similar values of IR/X even though their X-ray luminosities differ by a factor of over 60. (c) The IR/X ratio for starbursts has a mean value of about 1.3.

A caveat to determining a mean value of IR/X for general application to starbursts arises from the question of whether to include M 82. In Table 1, this source has unusually large values of IR/X. We noted in section 2 that the X-ray flux of M 82 can be greater by a factor of two when the variable source is in a high state. Such a situation would cause the IR/X of M 82 to be closer to that of the other starbursts. Since M 82 is only one of 9 regions in Table 1, we decided to include it when defining the mean IR/X for all starbursts, but we note the slight change that would occur without M 82.

[3] CIA is a joint development by the ESA astrophysics division and the ISOCAM consortium

[4] SIRTF Observer's Manual; http://sirtf.caltech.edu/SSC/obs/

The overall mean IR/X, for all redshifts z>1 and for all objects, is 1.33. This reduces to 1.08 without M 82. Wide field SIRTF "shallow" surveys at 24 μm, which can cover about 0.2 deg^2 per hour of observing, should reach sensitivities of 0.4 mJy. For the mean IR/X, a SIRTF starburst source of 0.4 mJy should have a typical CXO flux in the observed 0.5–2.0 keV soft band of 0.3×10^{-16} ergs s^{-1} cm^{-2}. The CXO can reach this flux limit for on-axis individual sources with $\sim$ 1 Ms of exposure (Brandt et al. 2001) and $\sim$ 2 Ms over a larger field (Alexander et al. 2003). We can conclude, therefore, that both CXO and SIRTF should be able to see the same starbursts for z>1. The number of such objects expected in a field depends significantly on models for luminosity function and the evolution of ultraluminous infrared galaxies. The models of Dole et al. (2003) predict about 200 starburst galaxies deg^{-2} with z>1.1, to the 0.4 mJy limit. This would correspond to 25 sources in the 450 arcmin^2 field covered by the CDF-N survey.

A major motivation for our attempt to determine IR/X for starbursts is to determine whether a comparison of SIRTF and CXO measurements can discriminate between starburst and AGN as the luminosity source for individual ULIRGs. This seems a reasonable expectation, because it is well established that nearby sources known to be dominated by AGN luminosity systematically have lower far-infrared to X-ray luminosity ratios than do starbursts (e.g. Levenson, Weaver, & Heckman 2001). For type 1 AGN, in which the broad line region and accretion disk can be observed directly, the luminosity in hard X-rays (which is what would be seen by CXO in the observer's frame at z>1) is typically 1000 times greater relative to the far-infrared luminosity than in starbursts. Even for type 2 AGN, in which the vicinity of the accretion disk is obscured from direct view, the analogous factor between AGN and starbursts is about 100, which implies that some hard X-rays from the AGN penetrate the obscuring material or escape via scattering from regions above the obscuring torus. Sources that are composite, with a type 2 AGN accompanied by comparably strong circumnuclear star formation, have X-ray to infrared ratios similar to starbursts. This is not surprising, since in such cases much of the X-ray and infrared luminosity arises from the starburst. While these results derived from considerations of far-infrared luminosity do not necessarily apply for SIRTF observations at 24 μm, it would be reasonable to conclude that an AGN is present in any object having IR/X lower than in pure starbursts.

Based on the results and trends in Table 1 and Figure 3, 95% of the starburst regions considered at the various redshifts have IR/X>0.2 (only 2 of the 45 entries in Table 1 are less than 0.2, and all are for the same low luminosity source). It is reasonable, therefore, to consider a limiting value of 0.2 as defining the lowest IR/X for a pure starburst. Any source with IR/X<0.2 can be considered with high probability to contain an AGN which contributes to the luminosity, because of the additional X-ray power. For a SIRTF 0.4 mJy source, this limiting IR/X means that a starburst should be fainter than a CXO flux of 2×10^{-16} ergs s^{-1} cm^{-2}. If the source were brighter than this in the CXO soft band, it can be reasonably classified as having some luminosity arising from an AGN rather than being purely a starburst.

This result does not mean, however, that any source with IR/X>0.2 can only be powered by a starburst. There is a category of obscured AGN in which the intrinsic X-ray luminosity is totally blocked to $\sim$ 10 keV by the obscuring material ($N_H > 10^{24}$ cm^{-2}) and only part of the scattered component may be seen. These are the "Compton Thick AGN" (e.g. Matt et al. 2000). In this case, IR/X might achieve high values compared to expectations for AGN because the absorbed X-ray luminosity would reappear as infrared luminosity. Risaliti, Maiolino, & Salvati (1999) and Levenson, Weaver, & Heckman (2001) conclude that known examples of Compton Thick AGN consistently have circumnuclear starbursts and suggest that these starburst regions could be the source of the material obscuring the AGN. If the AGN is a significant additional contributor to the infrared luminosity but not to the X-ray luminosity, the IR/X could even be greater than for a pure starburst.

We do not have an adequate sample of AGN to compare empirically with the IR/X measured for starbursts. There are only three AGN for which ISO and CXO data are available to analyse in the same way as the starburst sample; these are NGC 1068, the Circinus galaxy, and NGC 6240.[5] It happens that all three of these are obscured, Compton-thick AGN with circumnuclear starbursts (Levenson, Weaver, & Heckman 2001; Komossa et al. 2003; Lira et al. 2002; Sambruna et al. 2001) so it might be expected that these would be difficult objects to distinguish from pure starbursts based only on IR/X. For these objects, we measured the smallest feasible spatial region for applying the ISO and CXO spectra ($6'' \times 6''$) to isolate the AGN as much as possible in hopes of determining IR/X as it applies purely to an AGN component. Results for these three AGN are presented in Table 3. NGC 6240 falls within the AGN criterion already defined (IR/X<0.2) for most redshifts included, the Circinus galaxy is within this criterion at the highest redshift, but NGC 1068 would be confused with a starburst at any redshift based only on IR/X. This result indicates that IR/X does not provide an unambiguous criterion for a pure starburst. Nevertheless, if the infrared luminosity of a composite source (obscured AGN plus starburst) is dominated by the starburst, it would be appropriate to include such a source in the census of star formation derived from infrared surveys. We conclude, therefore, that the overlap in IR/X between pure starbursts and NGC 1068 or the Circinus galaxy should not discourage the use of IR/X as a primary sorting mechanism to distinguish between starbursts and AGN as the power source of ULIRGs discovered by SIRTF and Chandra.

Based on the foregoing analysis, what would be the most interesting and puzzling extragalactic sources to be revealed in comparisons of SIRTF and Chandra surveys? We have concluded empirically that sources with 3.0<IR/X<0.2 are starbursts or obscured AGN with circumnuclear starbursts. Objects with IR/X<0.2 have an additional source of X-ray emission beyond a starburst, so can be considered as having a dominant AGN. From Ta-

[5] The mid-IR data on NGC 1068 and NGC 6240 were presented in Le Floc'h et al. (2001) and Charmandaris et al. (1999) respectively, while the data on Circinus were retrieved from the ISO archive.

ble 1 and Figure 3, the upper bound for IR/X is about 4, if we ignore the single higher value for M82 for reasons discussed previously. Objects which would be anomalous according to any of the criteria defined would, therefore, be any objects with IR/X>4. If any such objects are found in comparisons of infrared and X-ray surveys, we recommend that they receive particular attention to determine their nature.

5. SUMMARY

Archival ISO CVF spectra and archival CXO spectra for several pure starbursts were evaluated to predict the ratio IR/X of SIRTF 24 μm flux densities (in mJy) to CXO total soft band fluxes (0.5–2.0 keV flux in units of $10^{-16}\,\mathrm{ergs\,s^{-1}\,cm^{-2}}$) which would be observed for spectrally similar starbursts seen at 1<z<3. For starbursts, IR/X was determined to have a mean value of 1.3 and falls between the extremes of 0.2 and 3.0. These empirical values for IR/X are suggested as an initial criterion for sorting ultraluminous infrared galaxies detected in SIRTF and CXO surveys into sources powered primarily by starbursts compared to those powered primarily by AGN. Sources with IR/X<0.2 probably have a dominant AGN; sources with IR/X>4 would be especially interesting, because they have no counterparts in the sample we have examined.

We acknowledge NASA for supporting this work through the Chandra X-ray Center (NAS 8-39073) and the SIRTF Infrared Spectrograph team (JPL 960803); AZ also acknowledges support by NASA LTSA grant NAG5-13056 and NASA grant G01-2120X. We thank an anonymous referee for helpful suggestions.

REFERENCES

Alexander, D. M., Aussel, H., Bauer, F. E., Brandt, W. N., Hornschemeier, A. E., Vignali, C., Garmire, G. P., & Schneider, D. P. 2002, ApJ, 568, L85
Alexander, D. M. et al. 2003, AJ, 126, 539
Alonso-Herrero, A., Rieke G. H, Rieke M.J., & Scoville, N. Z., 2000, ApJ, 532, 845
Barger, A. J., Cowie, L. L., & Richards, E. A. 2000, AJ, 119, 2092
Brandt, W. N. et al. 2001, AJ, 122, 2810
Cesarsky, C. J. et al. 1996, A&A, 315, L32
Charmandaris, V., Laurent, O., Mirabel, I. F., Gallais, P., Sauvage, M., Vigroux, L., Cesarsky, C., & Tran, D. 1999, Ap&SS, 266, 99
Charmandaris, V., Stacey, G. J., & Gull, G. 2002, ApJ, 571, 282
Chary, R., & Elbaz, D. 2001, ApJ, 556, 562
Clements, D. L., McDowell, J. C., Shaked, S., Baker, A. C., Borne, K., Colina, L., Lamb, S. A., & Mundell, C. 2002, ApJ, 581, 974
Della Ceca, R. et al. 2002, ApJ, 581, L9
Dole, H., Lagache, G., & Puget, J.-L. 2003, ApJ, 585, 617
Elbaz, D., Cesarsky, C. J., Chanial, P., Aussel, H., Franceschini, A., Fadda, D., & Chary, R. R. 2002, A&A, 384, 848
Fabbiano, G., Zezas, A., & Murray, S. S. 2001, ApJ, 554, 1035
Fabbiano, G., Zezas, A., King, A. R., Ponman, T. J., Rots, A., & Schweizer, F. 2003, ApJ, 584, L5
Fan, X. et al. 2001, AJ, 121, 54
Förster Schreiber, N. M., Sauvage, M., Charmandaris, V., Laurent, O., Gallais, P., Mirabel, I. F., & Vigroux, L. 2003, A&A, 399, 833
Gallais, P., Laurent, O., Charmandaris, V., Rouan, D., Mirabel, I. F., Sauvage, M., Tran, D., & Vigroux, L. 1998, in "The Universe as seen by ISO", ESA SP-427, p. 881
Gehrz, R. D., Sramek R. A., & Weedman, D. W. 1983, ApJ, 267, 551
Hauser, M. et al. 1998, ApJ, 508, 25
Hornschemeier, A. E. et al. 2001, ApJ, 554, 742
Hornschemeier, A. E., Brandt, W. N., Alexander, D. M., Bauer, F. E., Garmire, G. P., Schneider, D. P., Bautz, M. W., & Chartas, G. 2002, ApJ, 568, 82
Iwasawa, K., Matt, G., Guainazzi, M., & Fabian, A.C. 2001, MNRAS, 326, 894
Kaaret, P., Prestwich, A. H., Zezas, A., Murray, S. S., Kim, D.-W., Kilgard, R. E., Schlegel, E. M., & Ward, M. J. 2001, MNRAS, 321, L29
Komossa, S., Burwitz, V., Hasinger, G., Predehl, P., Kaastra, J. S., & Ikebe, Y. 2003, ApJ, 582, L15
Lagache, G., Dole, H., & Puget, J.-L. 2003, MNRAS, 338, 555
Le Floc'h, E., Mirabel I.F., Laurent, O., Charmandaris, V., Gallais, P., Sauvage, M., Vigroux, L., & Cesarsky, C., 2001, A&A, 367, 487
Levenson, N. A., Weaver, K. A., & Heckman, T. M. 2001, ApJ, 550, 230
Lira, P., Ward, M. J., Zezas, A., & Murray, S. S. 2002, MNRAS, 333, 709
Matsumoto, H., Tsuru, T. G., Koyama, K., Awaki, H., Canizares, C. R., Kawai, N., Matsushita, S., & Kawabe, R. 2001, ApJ, 547, L25
Matt, G., Fabian, A.C., Guainazzi, M., Iwasawa, K., Bassani, L. & Malaguti, G. 2000, MNRAS, 318, 173
Mirabel, I. F. et al. 1998, A&A, 333, L1
Moran, E. C., Lehnert, M. D., & Helfand, D. J. 1999, ApJ, 526, 649
Rieke, G. H., Lebofsky, M. J., Thompson, R. I., Low, F. J., & Tokunaga, A. T. 1980, ApJ, 238, 24
Risaliti, G., Maiolino, R., & Salvati, M. 1999, ApJ, 522, 157
Sambruna, R. M., Netzer, H., Kaspi, S., Brandt, W. N., Chartas, G., Garmire, G. P., Nousek, J. A., & Weaver, K. A. 2001, ApJ, 546, L13
Smith, H. E., Lonsdale, C. J., Lonsdale, C. J., & Diamond, P. J. 1998, ApJ, 493, 17
Stark, A. A., Gammie, C. F., Wilson, R. W., Bally, J., Linke, R. A., Heiles, C., & Hurwitz, M. 1992, ApJS, 79, 77
Strickland, D. K., Ponman, T. J. & Stevens, I. R., A&A, 1997, 320, 378
Sturm, E. et al. 1996, A&A, 315, L133
Vigroux, L. et al. 1996, A&A, 315, L93
Watson, M. G., Stanger, V., & Griffiths R. E. 1984, ApJ, 286, 144
Wilson, C. D., Scoville, N., Madden, S. C., & Charmandaris, V. 2000, ApJ, 542, 120
Xu, C. K., Lonsdale, C. J., Shupe, D. L., Franceschini, A., Martin, C., & Schiminovich, D. 2003, ApJ, 587, 90
Zezas, A. L., Georgantopoulos, I., & Ward, M. J. 1998, MNRAS, 301, 915
Zezas, A., Fabbiano, G., Rots, A. H., & Murray, S. S. 2002, ApJ, 577, 710
Zezas, A., Ward, M., Murray, S. S. 2003, ApJ, (submitted, astro-ph 0306375)

TABLE 1
SIRTF FLUX DENSITIES COMPARED TO CXO TOTAL FLUXES FOR STARBURSTS[a]

Region		Redshift (z)				
		1	1.5	2	2.5	3
	CXO band (keV):	1.0–4.0	1.25–5.0	1.6–6.0	1.75–7.0	2.0–8.0
Antennae - Knot A	f_x	530	399	342	315	284
	λ_{eff}	11.79	8.89	7.74	6.57	6.19
	f_ν	62	18	53	16	24
	IR/X	0.234	0.113	0.465	0.178	0.338
NGC 4038	f_x	325	271	242	224	206
	λ_{eff}	11.48	8.87	7.77	6.57	6.16
	f_ν	322	111	292	71	93
	IR/X	1.98	1.024	3.62	1.11	1.81
NGC 4039	f_x	529	398	341	314	282
	λ_{eff}	11.43	9.02	7.74	6.57	6.19
	f_ν	181	51	165	45	67
	IR/X	0.684	0.320	1.45	0.502	0.95
Antennae - Total	f_x	7220	7030	7220	7520	7760
	λ_{eff}	11.43	8.89	7.77	6.63	6.22
	fv	5660	1880	5250	1140	1410
	IR/X	1.57	0.670	2.18	0.529	0.730
Arp 220	f_x	441	527	617	704	783
	λ_{eff}	12.21	8.69	7.82	6.66	5.90
	f_ν	351	239	510	116	125
	IR/X	1.59	1.13	2.48	0.577	0.639
IC 694	f_x	751	855	930	1000	1050
	λ_{eff}	12.10	8.64	7.80	6.54	6.19
	f_ν	698	484	968	241	230
	IR/X	1.86	1.42	3.12	0.844	0.876
NGC 3690	f_x	3050	3040	3110	3200	3250
	λ_{eff}	11.79	8.84	7.80	6.60	6.01
	f_ν	1774	1091	1779	605	319
	IR/X	1.16	0.897	1.72	0.662	0.393
Arp 299 - Total	f_x	6390	6000	5950	6040	6040
	λ_{eff}	11.89	8.79	7.80	6.57	5.99
	f_ν	2238	1370	2753	863	429
	IR/X	0.70	0.571	1.39	0.500	0.284
M 82	f_x	56800	56700	57400	61800	61700
	λ_{eff}	11.74	8.74	7.71	6.63	6.13
	f_ν	68300	58400	139100	28200	42200
	IR/X	2.41	2.58	7.27	1.60	2.74

[a] f_x is the X-ray flux of the starburst region in the CXO band shown in units of 10^{-16} ergs s^{-1} cm^{-2}; λ_{eff} is the rest frame wavelength in μm that would be observed with the MIPS 24 μm filter at the redshift listed; f_ν is the rest-frame flux density of the starburst region in mJy (1 mJy = 10^{-26} ergs s^{-1} cm^{-2} Hz^{-1}) at λ_{eff}; IR/X would be the observed ratio of SIRTF 24 μm flux density in mJy to CXO soft band (0.5–2.0 keV) flux in units of 10^{-16} ergs s^{-1} cm^{-2} for a starburst having the spectral shape of this region and sufficient luminosity to be detected at the redshift listed.

Table 2
Luminosities of Starbursts

Region	IR/X (mean in Table 1)	L_x(2–8 keV) (ergs s^{-1})
Antennae - Knot A	0.27	2.1×10^{39}
NGC 4039	0.78	2.0×10^{39}
NGC 4038	1.91	1.5×10^{39}
Antennae - Total	1.14	5.6×10^{40}
Arp 220	1.28	5.4×10^{40}
IC 694	1.62	2.2×10^{40}
NGC 3690	0.97	6.8×10^{40}
Arp 299 - Total	0.69	1.3×10^{41}
M 82	3.32	8.0×10^{39}

TABLE 3
SIRTF FLUX DENSITIES COMPARED TO CXO TOTAL FLUXES FOR AGN[a]

AGN		Redshift (z)				
	CXO band (keV):	1 1.0–4.0	1.5 1.25–5.0	2 1.6–6.0	2.5 1.75–7.0	3 2.0–80
Circinus	f_x	15800	22600	31500	73100	85000
	λ_{eff}	11.79	9.04	7.69	6.68	5.86
	f_ν	12450	3930	8040	4360	2780
	IR/X	1.58	0.435	0.77	0.209	0.131
NGC 1068	f_x	28000	21600	20500	30300	31100
	λ_{eff}	11.63	9.12	7.74	6.63	5.77
	f_ν	33700	19000	18300	13400	10900
	IR/X	2.41	2.20	2.68	1.55	1.41
NGC 6240	f_x	4660	5590	6480	10200	11000
	λ_{eff}	11.95	8.79	7.79	6.65	5.93
	f_ν	454	330	625	198	120
	IR/X	0.20	0.15	0.29	0.068	0.044

[a] f_x is the X-ray flux of the AGN in the CXO band shown in units of 10^{-16} ergs s^{-1} cm^{-2}; λ_{eff} is the rest frame wavelength in μm that would be observed with the MIPS 24 μm filter at the redshift listed; f_ν is the rest-frame flux density of the AGN in mJy (1 mJy = 10^{-26} ergs s^{-1} cm^{-2} Hz^{-1}) at λ_{eff}; IR/X would be the observed ratio of SIRTF 24 μm flux density in mJy to CXO soft band (0.5–2.0 keV) flux in units of 10^{-16} ergs s^{-1} cm^{-2} for an AGN having the spectral shape of this AGN and sufficient luminosity to be detected at the redshift listed.

FIG. 1.— ISO 15 μm images of the galaxies in our sample obtained using the broadband LW3 (12–18μm) filter of ISOCAM. The individual areas from where the mid-IR spectra were extracted are indicated with boxes. The same areas were used to extract the X-ray spectra from CXO-ACIS observations. For NGC 4038/39, the large box is Antennae-Total, the upper small black box is NGC 4038, the lower small black box is NGC 4039, and the white box is Antennae-Knot A. For Arp 299, the large box is Arp 299-Total, the medium box is NGC 3690 and the smallest box is IC 694.

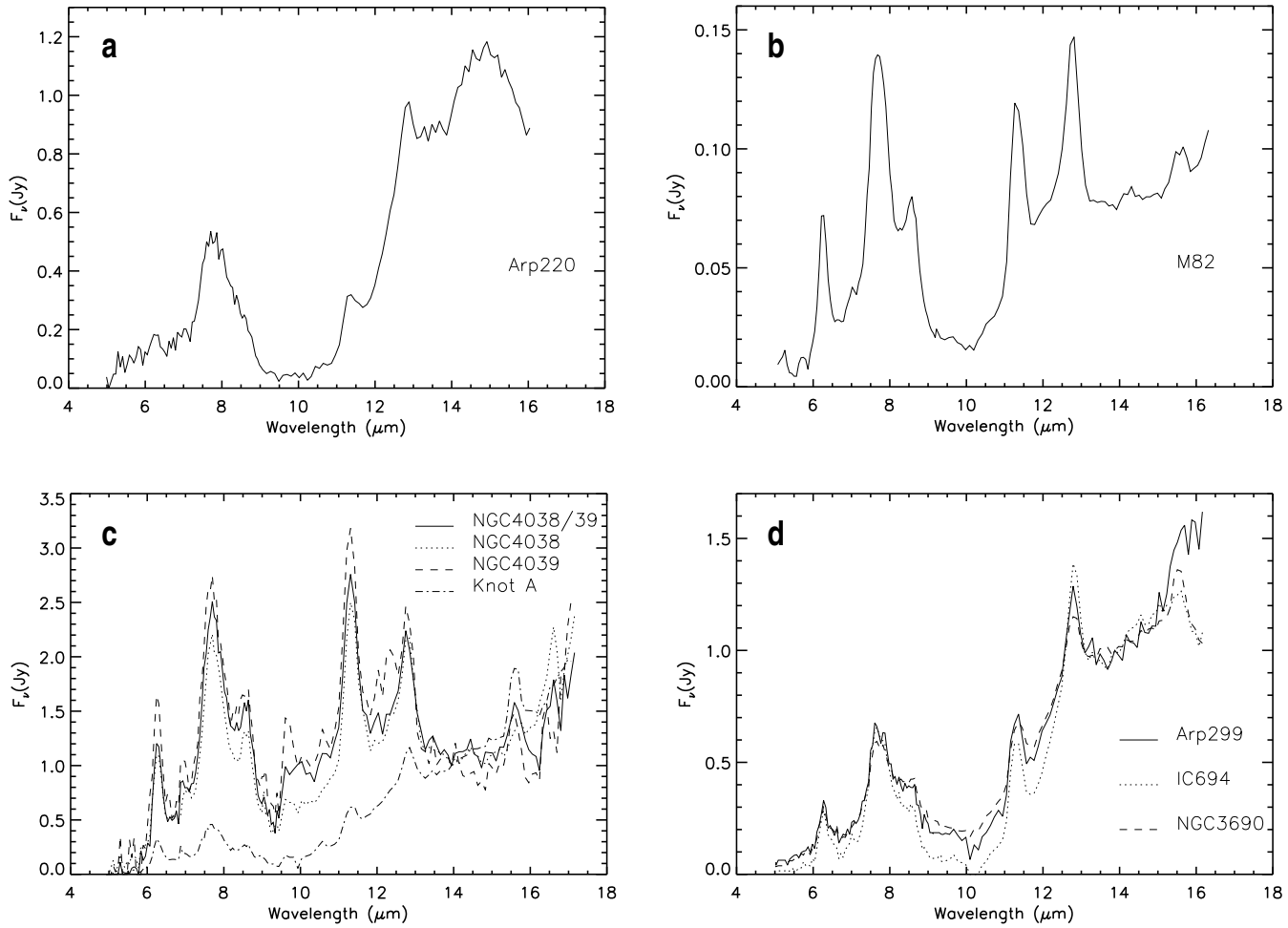

FIG. 2.— a) Rest frame ISOCAM/CVF 5–16.3 μm spectrum of Arp 220. b) As in a) but for M 82. c-d) As in a) but for the various regions of NGC 4038/39 and Arp 299 respectively. Those regions are marked in Figure 1. Note that in figures 2c) and 2d) the spectra have been normalized to unity at 14 μm. The scale factors by which each spectrum must be multiplied in order to retrieve the exact flux density detected are: NGC 4038=0.138, NGC 4039=0.060, Knot A=0.116, NGC 4038/39=2.153, IC 694=1.536, NGC 3690=2.099, and Arp 299=4.340.

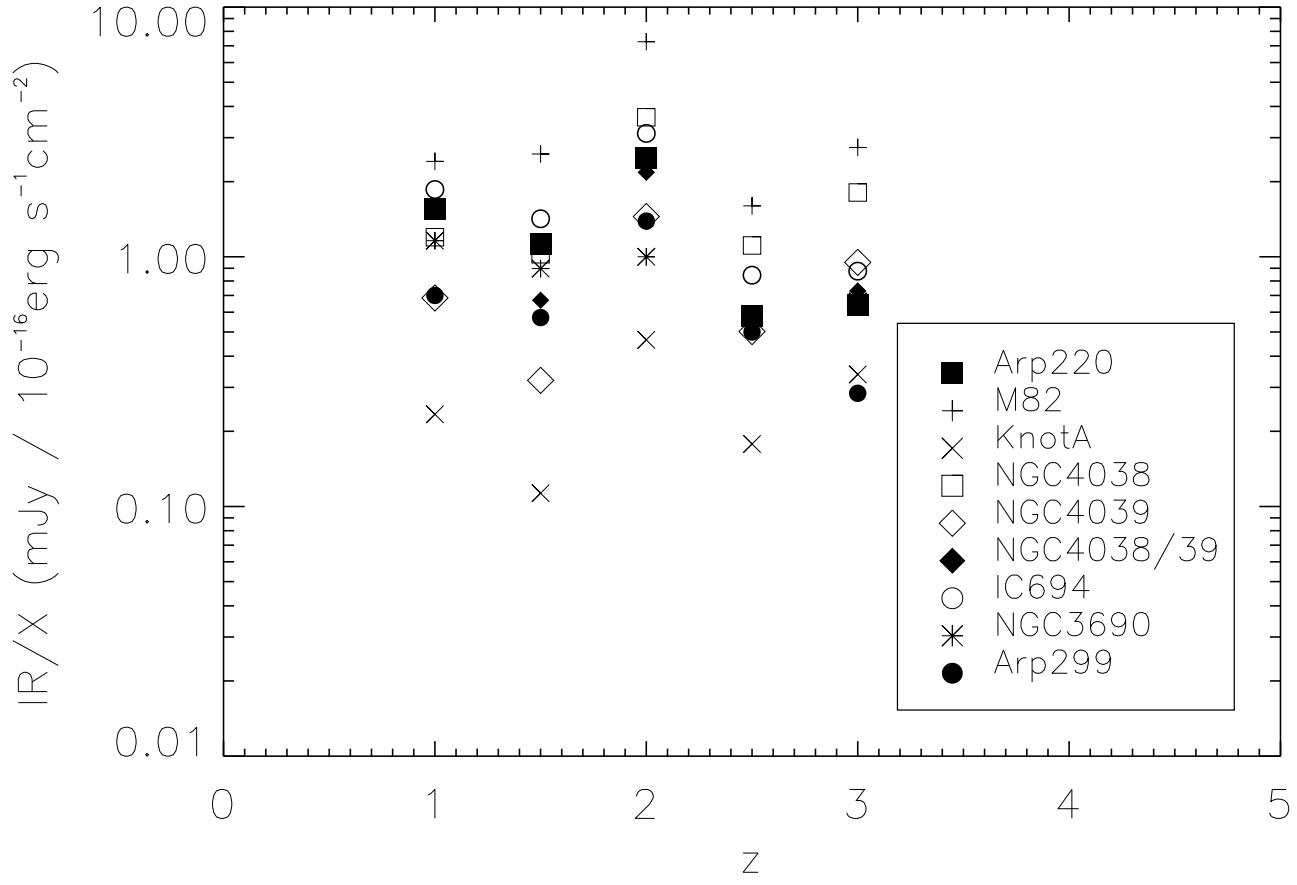

FIG. 3.— The IR/X ratio for the various starburst regions of the sample as a function of redshift.

This figure "f1.jpg" is available in "jpg" format from:

http://arXiv.org/ps/astro-ph/0309467v1